Figure S1. Wind roses based on a) surface measurements and radiosonde measurements at b) 2.5, c) 3.0, and d) 4.5 km MSL between October 23 and December 15.
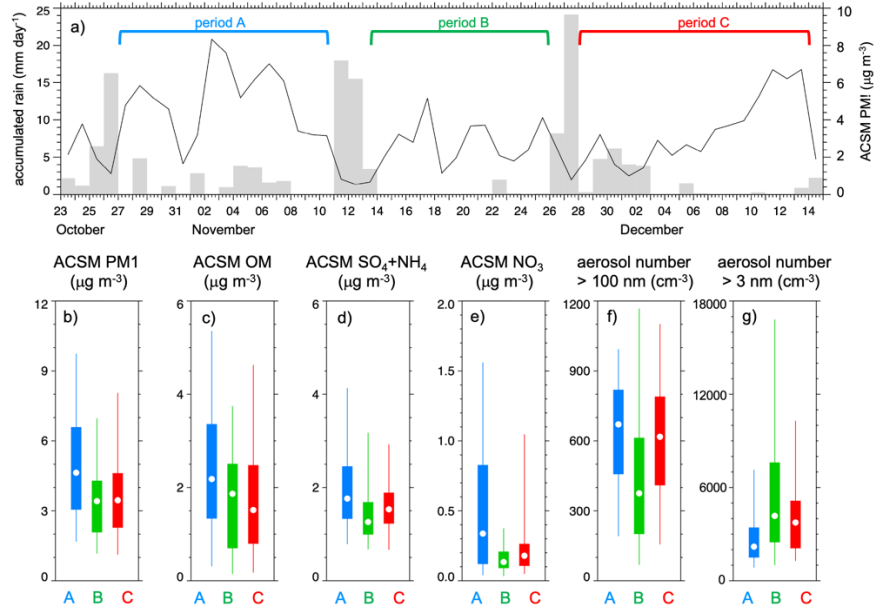
Figure S2. a) Daily averages of ACSM PM1 concentrations and accumulated rain from the optical rain gauge instrument between October 23 and December 15 that define periods A, B, and C, along with percentiles of b) PM1, c) OM, d) SO_4+NH_4, e) NO_3, f) aerosol number > 100 nm and g) aerosol number > 3 nm during periods A, B, and C.
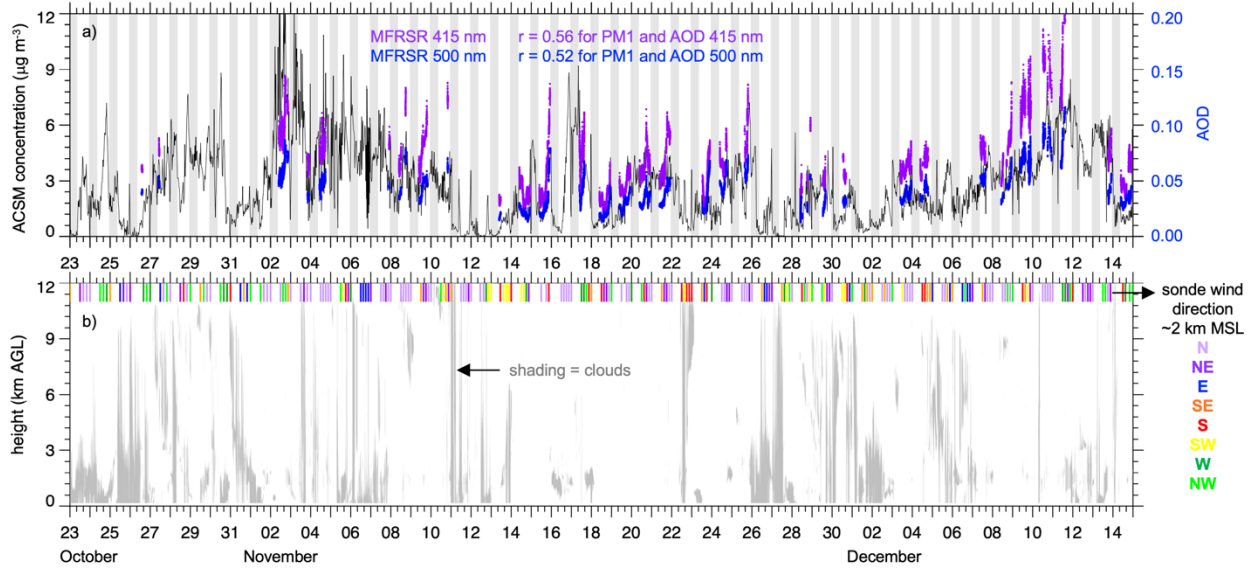
11

12 Figure S3. Time series of a) ACSM PM1 concentration and AOD at 415 and 500 nm and b) vertical
13 distribution of clouds from KAZR-ARSCL. Color bar at the top of b) denotes radiosonde
14 wind directions at ~2 km MSL.

15
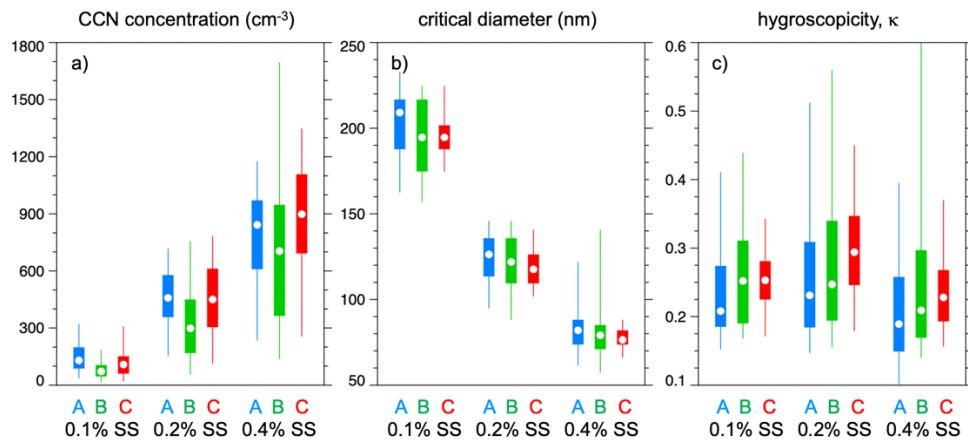
16

17 Figure S4. Percentiles of a) CCN concentration, b) critical diameter, and c) hygroscopicity during
18   periods A, B, and C for 0.1, 0.2 and 0.4% supersaturations.

19
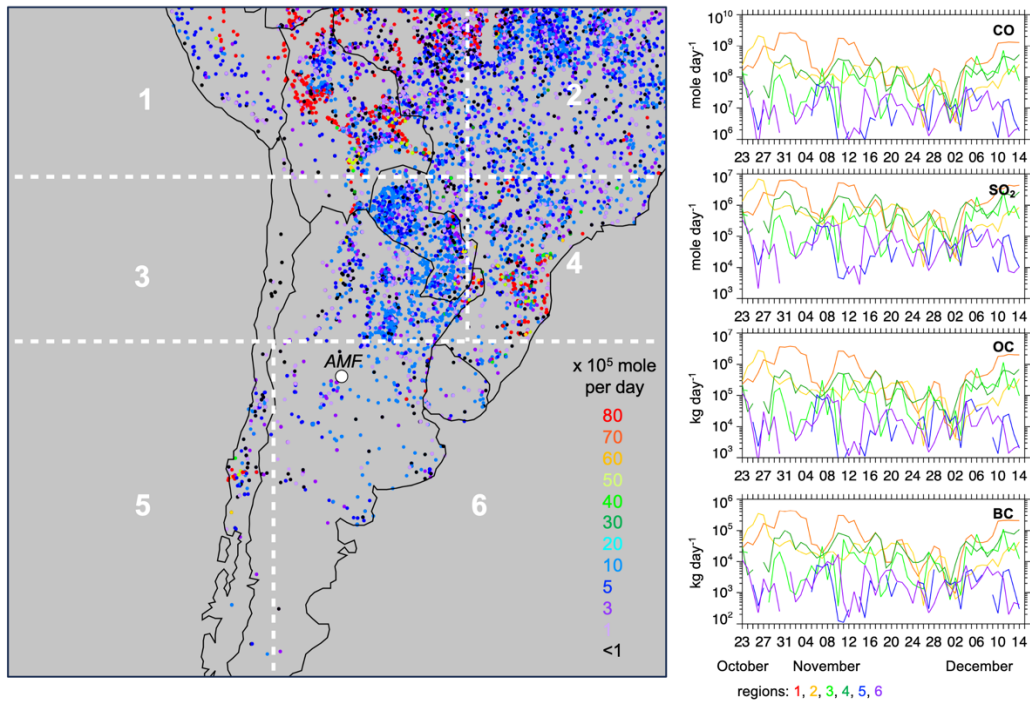
20

21   Figure S5.   FINN emissions of CO from individual fires between October 23 and December 15 (left
22   panel) over South America and daily variation in total CO, SO_2, OC, and BC emissions (right
23   panels) defined by the six regions over South America.

24
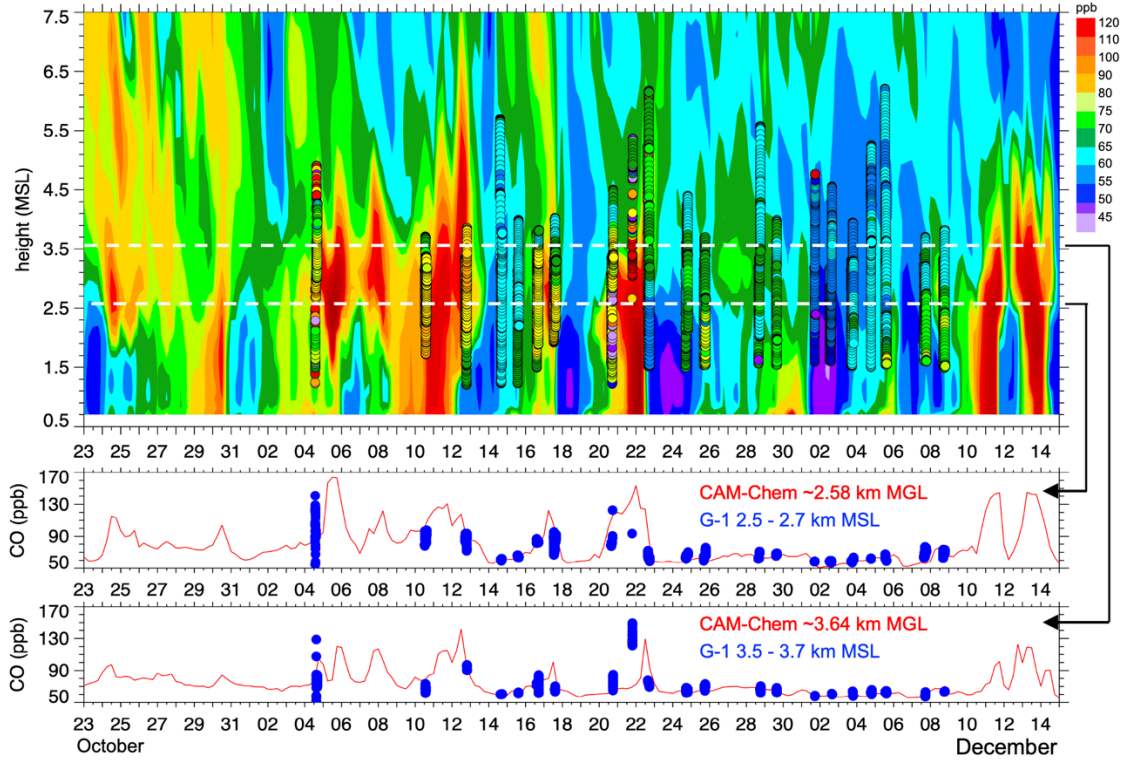
25

26 Figure S6. Temporal variation of CAM-Chem simulated CO profiles over the AMF site along with
27   aircraft measurements (dots). Lower two panels depict time series of observed (blue dots) and
28   simulated (red line) CO at ~2.58 and ~3.64 km MSL.

29

30
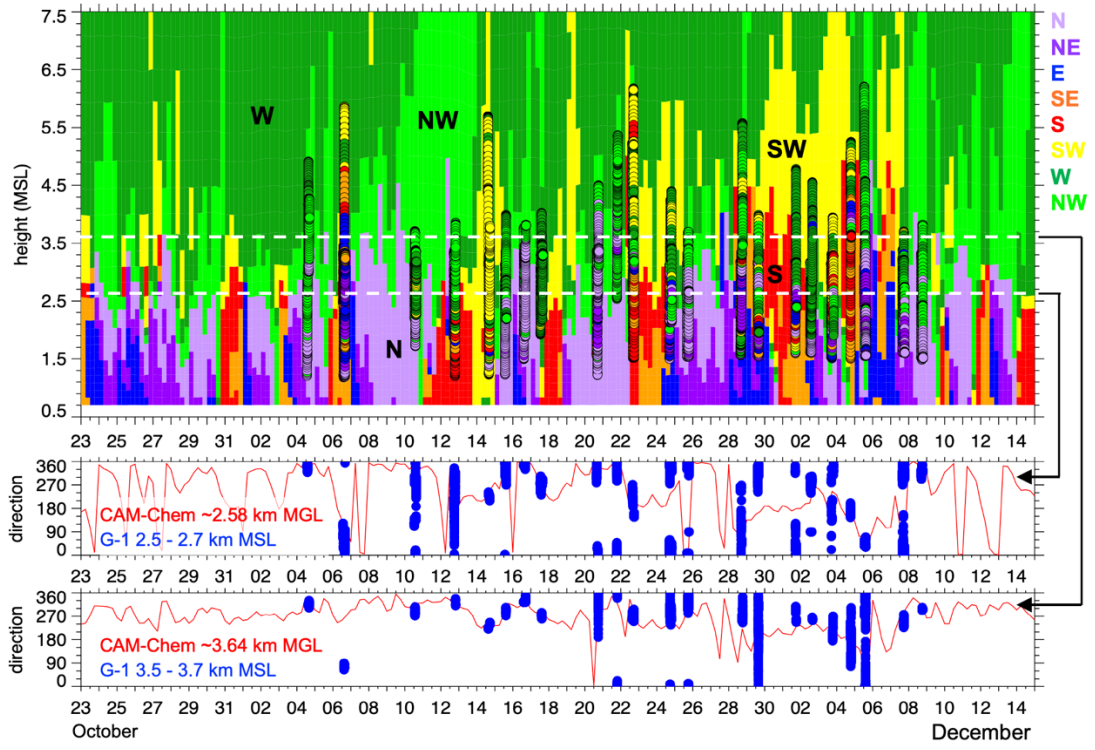
Figure S7.   Same as Fig. S6, except for wind direction.

32

33
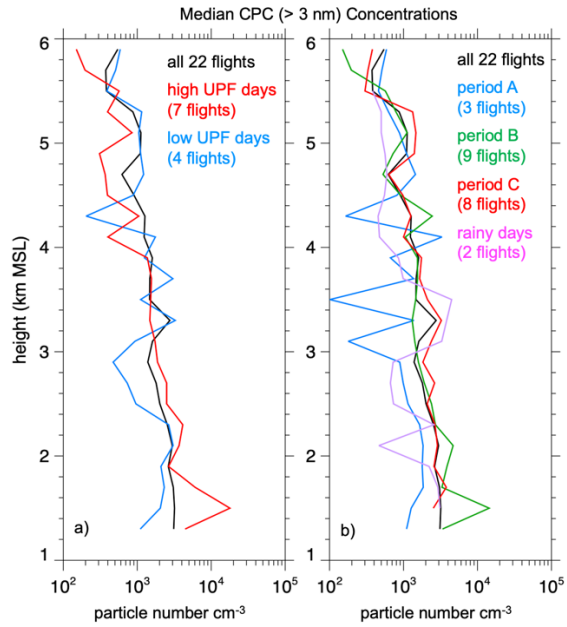
Figure S8.   Profiles of median particle number concentrations (> 3 nm) for all aircraft flights and flights
divided into a) low and high UPF days and b) periods A, B, and C.

34
35
36

37
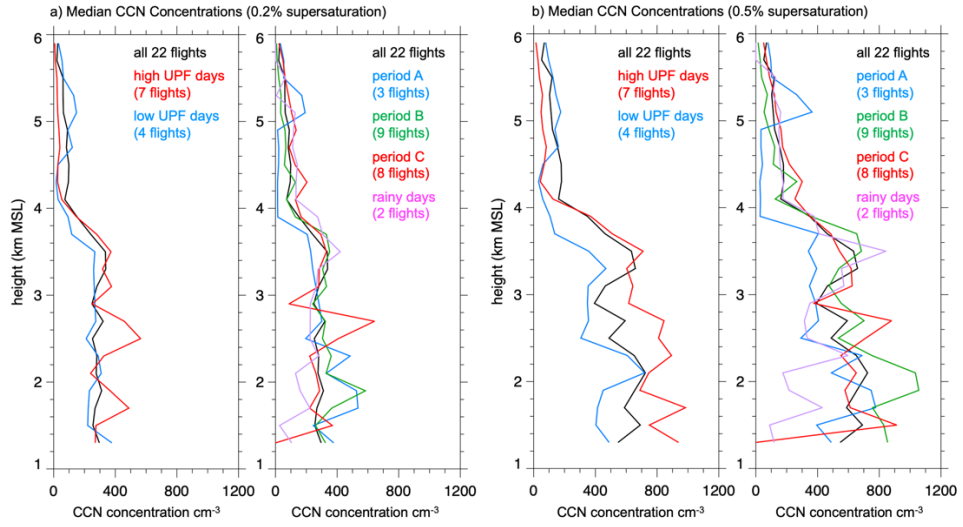
Figure S9.   Same as Fig. S5, except for CCN concentrations at a) 0.2% and b) 0.5% supersaturations.

39
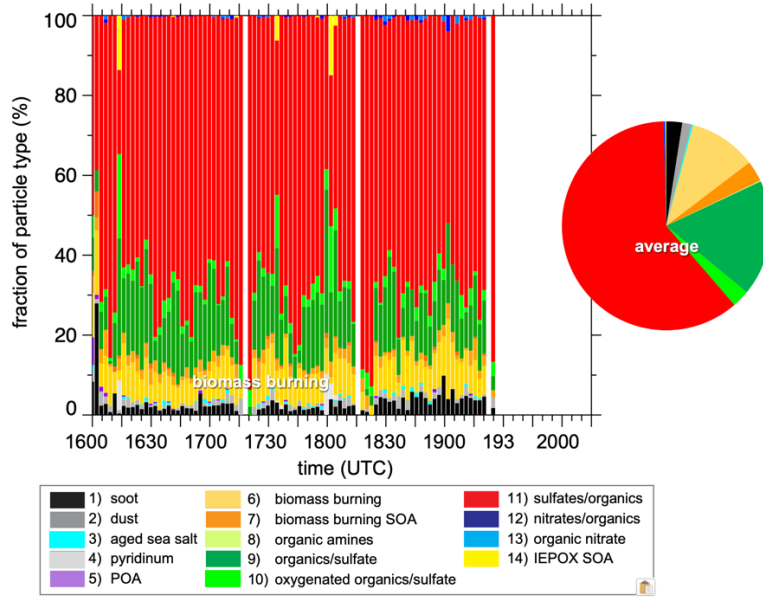
41 Figure S10. Particle classes derived from the aircraft miniSPLAT mixing state measurements on
42   December 3.